Lagerloef, G., (1995). Interdecadal variations in the Alaska Gyre, *J. Phys. Oceanogr*., **25**, 2242- 2258.

Mantua, N. J.; S.R. Hare, Y. Zhang, J.M. Wallace, and R.C. Francis (1997). A Pacific interdecadal climate oscillation with impacts on salmon production. *Bulletin of the American Meteorological Society* **78**: 1069–1079.

Overland, J.E., S. Salo, and J.M. Adams (1999). Salinity signature of the Pacific Decadal Oscillation. *Geophys. Res. Lett.*, **26**(9), 1337-1340.

Pielke Sr., R.A., C. Davey, D. Niyogi, S. Fall, J. Steinweg-Woods, K. Hubbard, X. Lin, M. Cai, Y.-K. Lim, H. Li, J. Nielsen-Gammon, K. Gallo, R. Hale, R. Mahmood, S.Foster, R.T. McNider, and P. Blanken, (2007): Unresolved issues with the assessment of multi-decadal global land surface temperature trends. *J. Geophys. Res*., **112**, D24S08, doi:10.1029/2006JD008229

Pokrovsky O.M., (2008). Relationship between the Atlantic Multidecadal Oscillation and the ice extent in Kara Sea. *CLIVAR Exchanges*, **46**, p.8-9.

Pokrovsky O.M., (2009) A coherency between the North Atlantic temperature nonlinear trend, the eastern Arctic ice extent drift and change in the atmospheric circulation regimes over the northern Eurasia. In a book *" Influence of Climate Change and Sub-Arctic Conditions on the Changing Arctic"* (Ed.J.C.J. Nihoul and A.G.Kostianoy), Springer Science Publ., 2009, p. 19-30.

Tikhonov, A.N. (1963), Inverse problem solution by regularization method. *Reports of Soviet Academy Sci.* v. **153**, N 1, p. 49-53 (in Russian, translated into English).

Trenberth, K. E. and Hurrell, J.W. (1994): Decadal atmosphere-ocean variations in the Pacific. *Climate Dynamics,* **9**, p. 303-319.

Wahba G. (1985), A comparison of GCV and GML for choosing the smoothing parameter in the generalized spline smoothing problem. *Ann. Statist*., v. **13**, p. 1378–1402, 1985.

Zhang, Y., J.M. Wallace, D.S. Battisti, (1997). ENSO-like interdecadal variability: 1900-93. *J. Climate,* **10**, p.1004-1020

How does El Niño Modoki affect the Australian monsoon?

Taschetto, A.S., A. Sen Gupta, C.C. Ummenhofer and M.H. England
Climate Change Research Centre (CCRC), University of New South Wales, Sydney, Australia
Corresponding author: a.taschetto@unsw.edu.au

1. Introduction

Over recent decades, a different flavor of El Niño has been observed in the tropical Pacific. These events, recently-termed El Niño Modoki, are characterized by warm SST anomalies in the central Pacific straddled by colder anomalies to either side (Ashok et al., 2007). Although the mechanisms behind El Niño Modoki episodes are still elusive, it is clear that their impacts on regional climate are distinct from those related to a canonical El Niño (Wang and Hendon, 2007).

In this study we assess the impacts of El Niño Modoki events on the Australian monsoon climate, using observations and simulations with an atmospheric general circulation model (AGCM).

2. Data and Methods

The following datasets are used in this study: (1) the global SST analysis from the Hadley Centre (HadISST1); (2) rainfall from the Australian Bureau of Meteorology (BoM); (3) winds, specific humidity and vertical velocity from the NCEP/NCAR Reanalysis. We confine our analysis to the more reliable post-satellite era, namely the period from 1979 to 2005.

The NCAR Community Atmospheric Model (CAM3) is used to assess the sensitivity of Australian rainfall to different locations of SST warming in the Pacific. The AGCM is forced with climatological monthly SST values and a superimposed 1ºC positive SST anomaly along the equatorial Pacific, bounded between 10ºN and 10ºS and longitudinally located in: (1) the eastern Pacific, from 120ºW to 80ºW; (2) the central-eastern Pacific, from 160ºW to 120ºW; (3) the central-western Pacific, from 160ºE to 160ºW; and, (4) the western Pacific, from 120ºE to 160ºE.

3. Results

Observations

The Modoki SST pattern appears as the second mode of interannual variability in an Empirical Orthogonal Function analysis over the tropical Pacific, accounting for approximately 12% of the total variance (Ashok et al., 2007). Taschetto and England (2009) have shown that when a Singular Value Decomposition (SVD) analysis is performed with seasonal Pacific SST and Australian rainfall data, the Modoki pattern actually appears as the leading mode of variability during austral autumn (MAM). It is associated with dry conditions across the continent, particularly to the north, during MAM.

The robustness of the SVD result was verified by the authors via composites of SST, rainfall, vertical velocity and velocity potential anomalies for the El Niño Modoki events in 1980, 1987, 1991, 1995 and 2003. A comparison of the impacts from Modoki events with the traditional El Niños of 1982, 1987 and 1997 revealed a marked difference over Australia: while classic El Niños are associated with a significant reduction in rainfall over northeastern and southeastern Australia during SON, the Modoki events appear to drive a large-scale decrease in rainfall over northwestern and northern Australia during MAM.

Associated with the Modoki SST pattern there is an upward motion through the deep troposphere centered at 180ºW, west of the rising air in the conventional ENSO-composite circulation. As a consequence, anomalous divergence is seen in the central-west Pacific that causes convergence and thus subsidence over South America and Indonesia, forming a double Walker Cell, as described by Ashok et al. (2007).

Interestingly, when the SVD and composite analyses are carried out for the austral summer season (DJF), northern Australia does not show strong dry conditions (not shown). This raises the question of why DJF rainfall does not show negative anomalies similar to MAM for the same Modoki signature. To address this question we examine the monthly evolution of rainfall during El Niño Modoki events.

Figure 1 depicts the December through March rainfall anomalies composited for El Niño Modoki events. Strikingly, it reveals the opposite signal in January and February compared to December and March. As a result, the SVD and composite analyses for the averaged summer season did not show a strong response as the negative and positive anomalies on individual months offset each other. This gives a false impression that the Modoki anomalies do not have a strong impact on Australian climate during the summer monsoon.

The reduced rainfall in December and March and increased rainfall in January and February is a robust signal across observed Modoki events. This can be seen in Figure 2 which shows the annual rainfall cycle averaged over northern Australia (12ºS-24ºS, 120ºE-135ºE) for individual Modoki years compared to the long-term climatology. The Modoki-related anomalies lead to a shortening of the monsoon season over northern Australia, with an associated intensification of precipitation in January and February. In other words, Modoki events can be associated with a late monsoon onset and an early monsoon termination over Australia.

To investigate the mechanisms behind the shorter and more intense burst of precipitation, we calculated the vertically integrated moisture flux from the surface to 500hPa and its associated divergence field. Figure 3a (page 38) reveals that intensified rainfall in February results from a stronger convergence of moisture caused by an anomalous cyclonic circulation over northwestern Australia. On the other hand, Australia experiences a divergence of moisture in March (Figure 3b) and thus drier-than-average conditions. The rainfall decrease in March is exacerbated by the subsidence of the western branch of the anomalous Walker circulation during Modoki events. However, anomalous subsidence is not evident over northern Australia in February (figure not shown).

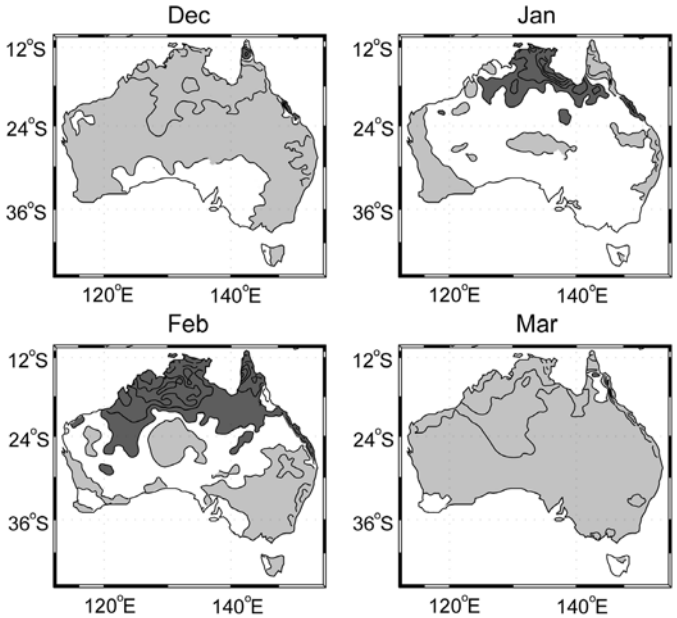

Figure 1. Rainfall anomaly composite for Modoki years from December to March (1979/1980, 1986/1987, 1990/1991, 1992/1993, 1994/1995 and 2002/2003). Positive values greater than 1mm/day are dark shaded and negative values are light shaded. Contour intervals are 1mm/day.

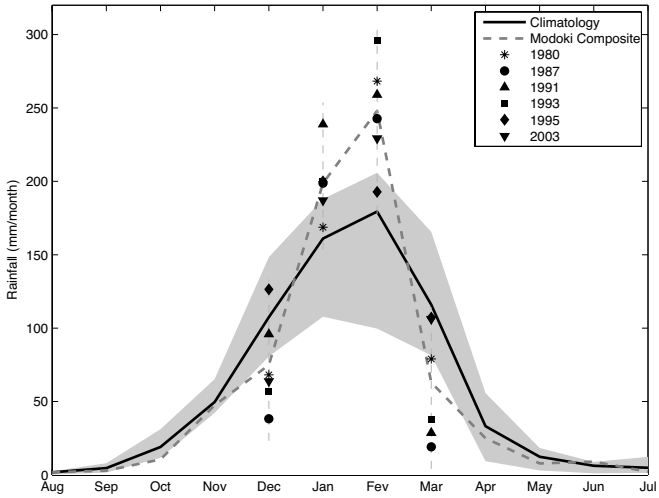

Figure 2. Annual cycle of rainfall in northwestern Australia. The black thick line represents the climatology and the dashed line indicates the mean anomalous behavior during El Niño Modoki years. Individual Modoki events from December to March are highlighted with symbols. Values outside the gray area are significant at the 95% level based on a Monte Carlo test.

The numerical experiments

The sensitivity of Australian rainfall anomalies to the location of warming along the equatorial Pacific is examined by applying warm SST anomalies at different tropical locations in numerical experiments (e.g. Fig. 3c,d). The idealized experiments show an overall rainfall increase in February and a decrease in March. The strongest rainfall response in February (wet) and March (dry) is seen when the positive SST anomaly forcing is located in the central-west Pacific (not shown). This corroborates Wang and Hendon (2007)'s finding that Australian climate is sensitive to the location of SST anomalies in the tropical Pacific. In addition, SST warming around the Dateline, typical of Modoki events, tends to impact more strongly on Australian rainfall, in the simulation, than the positive anomalies located in the east, as found during traditional El Niños.

The experiment forced with the SST warming in the central-west Pacific captures a convergence of moisture flux in February (Figure 3c) and a divergence over Australia in March (Figure 3d). This result suggests that a warming solely in the central-western Pacific may be sufficient to drive the monsoonal changes observed in Modoki years (Fig. 3a,b).

4. Conclusions

Changes in the magnitude and location of El Niño-induced-SST warming have significant implications for Australian rainfall. In this study we show for the first time that Modoki is associated with below-normal rainfall over northern Australia in December and March to May and intensified precipitation during January and February. This leads to a shorter and intensified monsoon season. This result appears very robust, occurring in almost all the Modoki events (for details, see Taschetto et al., 2009).

The increase in precipitation in January and February is caused by anomalous convergence of moisture flux onto the continent. The decreased rainfall in the other months

occurs via a divergence of moisture and the subsidence from the western branch of the altered Walker circulation during Modoki events. The reason why the subsidence is not seen in February remains unclear.

Using numerical experiments we showed that the Australian monsoon rainfall responds more strongly to a warming located in the central equatorial Pacific compared to a warming located in the east. The experiment with warming in the central-west Pacific simulated an anomalous convergence of moisture in February and an anomalous moisture divergence in March, suggesting that the Modoki–related SST warming is a key factor in modulating Australian monsoon variability.

References

Ashok, K., S. K. Behera, S. A. Rao, H. Weng, and T. Yamagata, 2007: El Niño Modoki and its possible teleconnection. *J. Geophys. Res*., **112** (C11007), doi:10.1029/2006JC003 798.

Taschetto, A. S. and M. H. England, 2009: El Niño Modoki impacts on Australian rainfall. *J. Clim*, **22**(11):3167-3174.

Taschetto, A. S., C. C. Ummenhofer, A. Sen Gupta and M. H. England, 2009: The effect of anomalous warming in the central Pacific on the Australian monsoon. *Geophys. Res. Lett*., **in press.**

Wang, G. and H. H. Hendon, 2007: Sensitivity of Australian rainfall to inter-El Niño variations. *J. Clim*., **20**, 4211–4226.

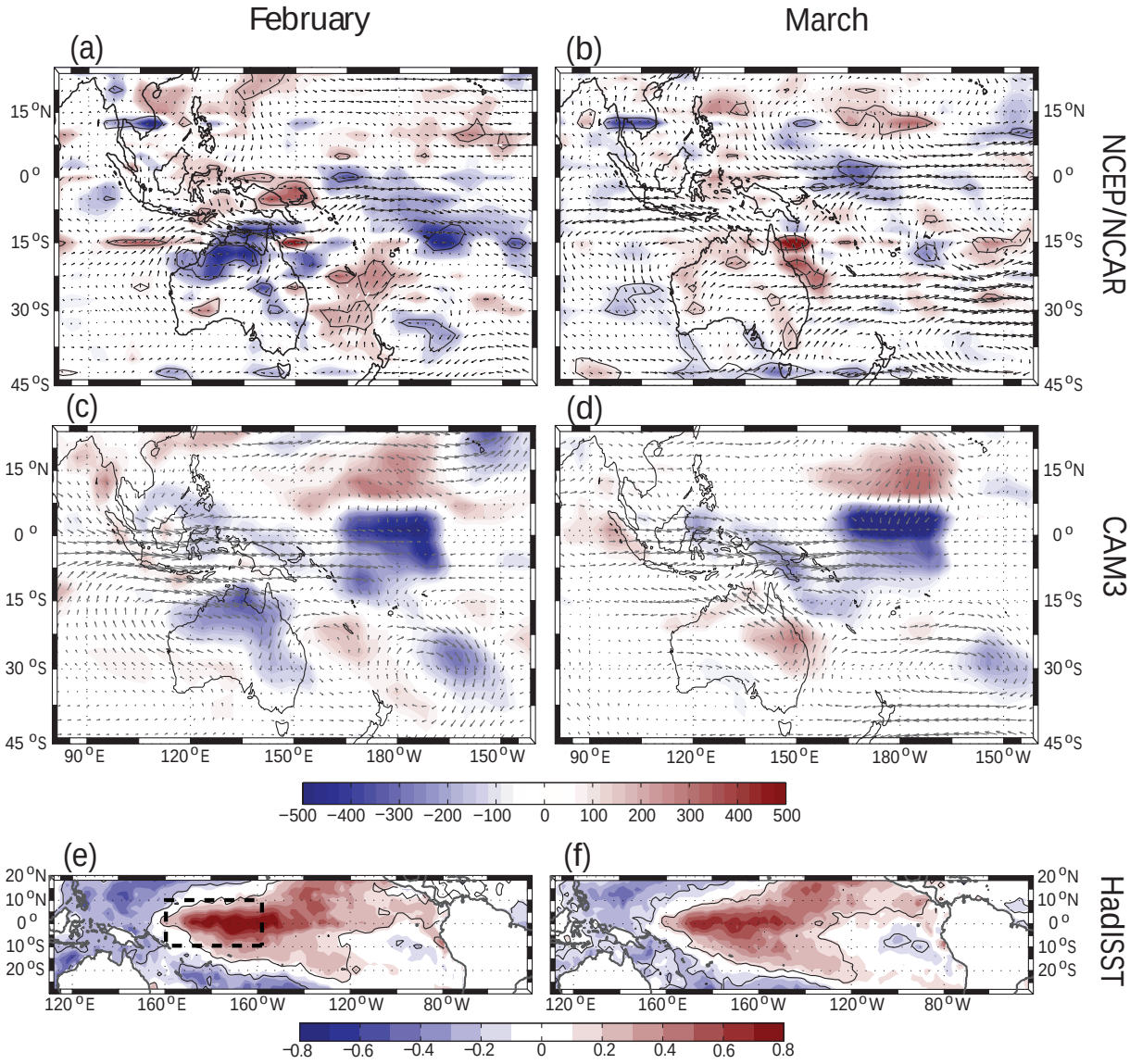

Figure 3. Composite anomalies of (a-d) moisture flux (kg m^{-1} s^{-1}), divergent moisture flux (kg s^{-1}) and (e-f) SST (Celsius) during Modoki events in February (left panels) and March (right panels). (a-b) NCEP/NCAR reanalysis, (c-d) NCAR CAM3 model and (e-f) HadISST. Areas within the thin black contours are significant at the 95% level. The solid black box in (e) represents the area where the SST anomaly was imposed to force the central-west Pacific experiment. The maximum vector length is 5 kg m^{-1} s^{-1}.